High Conductivity Perfluorosulfonic Acid Nanofiber Composite Fuel-Cell Membranes

Jonghyun Choi,[b] Ryszard Wycisk,[b] Wenjing Zhang,[a] Peter N. Pintauro,*[a] Kyung Min Lee,[b] and Patrick T. Mather[c]

There is a need for polymeric hydrogen/air fuel-cell membranes that can efficiently conduct protons at moderate to high temperatures for wet and dry gas feeds. The US Department of Energy (DOE), for example, set an exceedingly stringent preliminary target for membrane conductivity, 0.10 S cm^{-1} at 120 °C and 50 % relative humidity (RH).[1] Herein, we describe the fabrication and basic properties of one membrane that exhibits outstanding proton conductivity over a wide range of humidity conditions at temperatures of 80 °C and 120 °C. The membrane is based on a nanofiber network composite design[2] with precise topological separation of the proton transporting and mechanically reinforcing polymer components. This desirable morphology is created via electrospinning, an electrostatic fiber processing technique that has been known for more than one hundred years and underwent a renaissance in the early 1990s, mainly due to the work of Reneker et al.[3, 4]

The use of electrospinning for membrane and porous filter fabrication is not yet widespread, but interest in this technique is growing. Nanofiber air filters with highly desirable retention characteristics have recently been commercialized.[5, 6] Electrospinning of ionic polymers, on the other hand, is quite new and the data on these systems are very scarce.

The present implementation of electrospinning, leading to a functional proton conducting membrane, is unique and involves a sequence of four processing steps: 1) electrospinning a proton conductive blend containing a negatively charged polymer and a sulfonated molecular silica (silsesquioxane) to create a nanofiber mat, 2) welding of intersecting nanofibers to improve the connectivity of the protonic pathways, 3) compacting the mat to increase the volumetric density of the proton conductive fibers, and 4) impregnating the processed nanofiber network with an inert, hydrophobic (uncharged) polymer to fill the pores between fibers, reinforcing the membrane, and limiting ionomer swelling.

The new ion-exchange membrane differs from alternative approaches, such as those based on block copolymers,[7, 8] in that it combines two separate materials: one for proton conduction and the other as a reinforcement and for stabilizing ionomer swelling, which allows for better control of the nanostructure and properties. Thus, the submicron component (i.e., the "mixing" of the constituent electrospun nanofibers and inert, uncharged polymer matrix) produces a co-continuous morphology similar to that of a polymer blend at the point of phase inversion.

Initial experiments focused on the highly charged 825 equivalent weight (EW) perfluorosulfonic acid (PFSA) polymer from 3M Corporation, with an ion-exchange capacity (IEC) of 1.21 mmol g^{-1} (i.e., 33 % more $-SO_3H$ proton exchange groups per unit weight than commercially available 1100 EW Nafion).

Data on electrospinning of PFSA polymers is sparse and limited to Nafion.[9–11] Researchers have been unable to electrospin neat Nafion fibers from a Nafion/alcohol solution due to the polymer's rod-like micellar morphology and the lack of sufficient chain entanglements. Electrospinning was only possible when a carrier polymer, poly(acrylic acid) or poly(ethylene oxide), was added to the Nafion solution at a high concentration (15–30 wt %).

The carrier approach, utilizing poly(acrylic acid) (PAA), was adopted in the present study, with a focus on minimizing the PAA content of the PFSA nanofibers. Solutions of 3M PFSA/PAA in 1-propanol/water (2:1 w/w) solvent containing 5–15 wt % total polymer and 5–50 wt % PAA with respect to PFSA were electrospun. Scanning electron microscopy (SEM) images of the resultant mats and the average fiber diameters are shown in Figure 1. Electrospinnability was enhanced and the average fiber diameter increased as the PAA content and the total polymer concentration of the spinning solution increased. Electrosprayed droplets formed with a 5 % solution containing 5 % PAA due to insufficient number of polymer chain entanglements, whereas a 15 % solution with 50 % PAA could not be spun due to its very high viscosity. Only 5 % PAA was needed to electrospin well-formed PFSA fibers when the total polymer concentration was 15 wt %. This is a significant drop in carrier concentration, as compared to all prior reports (due to our optimization of the electrospinning conditions).

To further enhance proton conduction in the final nanofiber-based membrane, a 3-component system was electrospun, containing 60 % 825 EW PFSA, 5 % PAA, and 35 % sulfonated octaphenyl polyhedral silsesquioxane (sPOSS, with an IEC of 4.8 mmol g^{-1}; molecular structure is shown in Figure 2). sPOSS was selected based on a prior report showing a positive influence of a similar compound on the proton conductivity of a non-fibrous direct methanol fuel-cell membrane.[12]

Electrospun PFSA/PAA (95:5) and PFSA/sPOSS/PAA (60:35:5) nanofiber mats were further processed by heating to 140 °C

[a] Dr. W. Zhang, Prof. P. N. Pintauro
    Department of Chemical and Biomolecular Engineering
    Vanderbilt University, Nashville, TN 37235 (USA)
    Fax: (+1) 615-343-7951
    E-mail: peter.pintauro@vanderbilt.edu

[b] Dr. J. Choi, Dr. R. Wycisk, Dr. K. M. Lee
    Department of Chemical Engineering
    Case Western Reserve University, Cleveland, OH 44106 (USA)

[c] Prof. P. T. Mather
    Department of Biomedical and Chemical Engineering
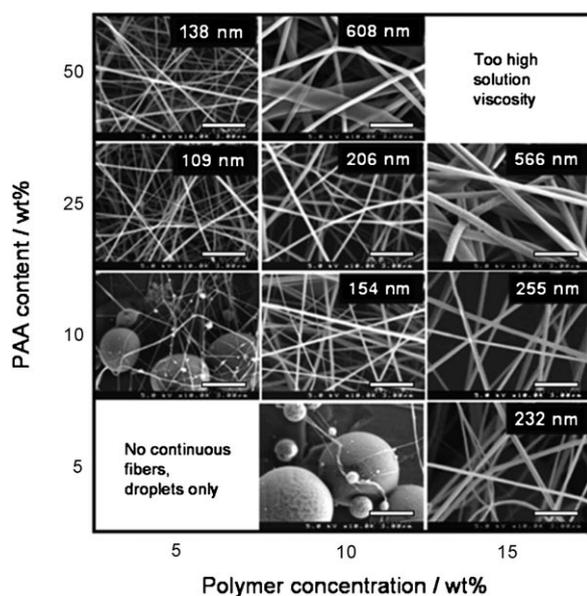   Syracuse University, Syracuse, NY 13244 (USA)

Figure 1. Scanning electron micrographs of electrospun nanofibers or electrosprayed droplets of PFSA/PAA with varied PFSA/PAA ratios (95:5 to 50:50 w/w) and polymer concentrations (5–15 wt %). The average fiber diameter and scale bar (3 μm) for each condition are shown in the insert.
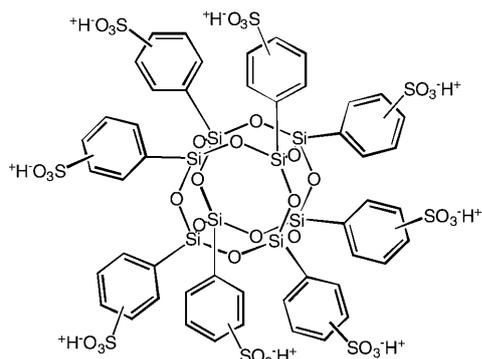

Figure 2. Molecular structure of fully sulfonated octaphenyl polyhedral oligomeric silsesquioxane (sPOSS) with an IEC of 4.8 mmol g^{-1}.
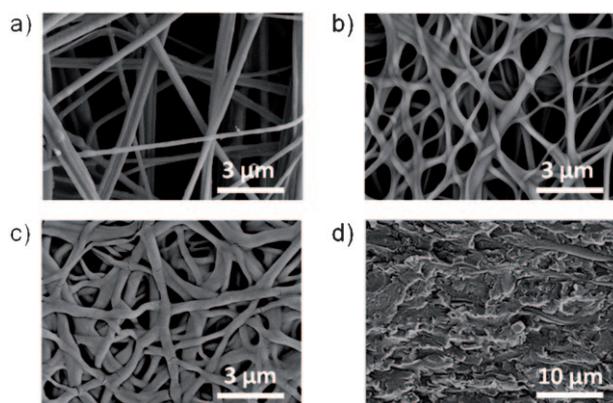

Figure 3. Scanning electron micrographs of a PFSA/sPOSS/PAA (60:35:5 w/w/w) nanofiber mat: a) initial electrospun mat surface with 0.20 fiber volume fraction (275 nm average fiber diameter), b) annealed/welded mat surface with 0.35 fiber volume fraction, c) annealed/welded and densified mat surface with 0.74 fiber volume fraction, and d) mat impregnated with Norland Optical Adhesive NOA 63 (cross-section, freeze-fractured) with 0.74 fiber volume fraction.

Table 1. Proton conductivity (S cm^{-1}) of membranes at 120 °C.

	20 % RH	50 % RH	90 % RH
Nanofiber membrane[a]	0.021	0.107	0.498
Nafion 212	0.006	0.039	0.185
[a] PFSA/sPOSS/PAA (60:35:5 w/w/w) with NOA 63 filling the interfiber voids.			

and holding for 5 min to anneal the PFSA and to weld fibers at their intersection points. Mechanical compression was used to increase the volume fraction of proton conductive nanofibers in an annealed mat from approximately 0.35 to 0.71–0.74. For the final processing step, a nanofiber mat was impregnated with an inert liquid prepolymer, Norland Optical Adhesive (NOA 63), and then exposed to UV light for NOA 63 curing. Scanning electron micrographs of the PFSA/sPOSS/PAA nanofiber mat at each processing step prior to impregnation are shown in Figure 3 (a–c). The cross-section of a freeze-fractured impregnated membrane is presented in Figure 3 d. Excellent void filling by NOA 63 is evident.

Membranes were characterized in terms of proton conductivity and water vapor sorption. The proton conductivity of the nanofiber composite membrane at 120 °C and 20 %, 50 %, and 90 % RH is contrasted with that of Nafion 212 in Table 1 (additional proton conductivity data can be found in the Supporting Information).

The PFSA/sPOSS/PAA nanofiber composite membrane exhibited an extraordinarily high conductivity of 0.107 S cm^{-1} at 120 °C and 50 % RH, among the highest reported conductivity in the open literature and exceeding the US DOE membrane performance target. Through-plane conductivities were not measured in the present study, but they are expected to be the same as the in-plane results, based on SEMs which showed an isotropic nanofiber structure and from prior studies with a sulfonated polysulfone nanofiber composite membrane, where identical in-plane and through-plane conductivities were measured.[2] The variation of in-plane proton conductivity with relative humidity at 80 °C is shown in Figure 4 for three membranes: a PFSA/sPOSS/PAA (60:35:5 w/w/w) nanofiber composite membrane, a PFSA nanofiber composite membrane (no sPOSS) and Nafion 212 (as a reference). The conductivity of the PFSA/sPOSS/PAA nanofiber composite membrane at 80 °C and 50 % RH (0.083 S cm^{-1}) was 2.4-times greater than that of the PFSA nanofiber composite membrane (0.034 S cm^{-1}) and three-times greater than Nafion 212 (0.028 S cm^{-1}). The calculated activation energy for proton conduction in the PFSA/sPOSS/PAA nanofiber composite membrane at 50 % RH (10.6 ± 0.71 kJ mol^{-1}) and 90 % RH (12.2 ± 0.98 kJ mol^{-1}) were near those of Nafion 212 (11.3 ± 0.24 kJ mol^{-1} at 50 % RH and 13.8 ± 0.01 kJ mol^{-1} at 90 % RH), indicating no unique or distinguishable proton conduction mechanism (see the Supporting Infor-
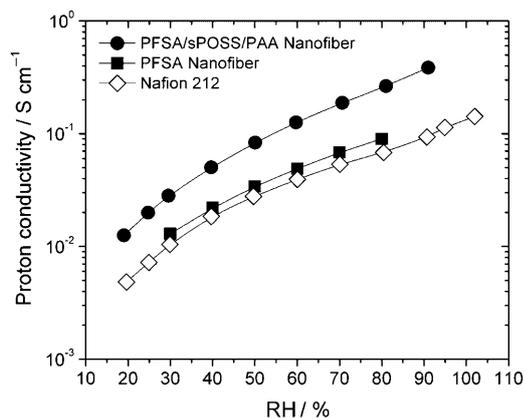
Figure 4. In-plane membrane proton conductivity as a function of relative humidity at 80 °C. PFSA/sPOSS/PAA (60:35:5 w/w/w) nanofiber composite membrane (0.74 fiber volume fraction), PFSA nanofiber composite membrane (0.71 volume fraction), and Nafion 212.

Figure 5. Hydration number vs relative humidity at 80 °C for neat sPOSS, a PFSA/sPOSS/PAA nanofiber composite membrane (825 EW PFSA, with a fiber volume fraction of 0.74), a PFSA nanofiber composite membrane (no sPOSS, 825 EW PFSA, 0.71 fiber volume fraction), a homogeneous PFSA/PAA film, and commercial Nafion 212.

mation for Arrhenius plots). Unfortunately, sPOSS material leached out of a nanofiber composite membrane after immersion in room temperature water. Over a period of 12 h, approximately 95 % of the sPOSS was lost, as determined from weight change measurements. Thus, for the eventual use of this membrane in a H_2/air fuel cell, either a method of stabilizing sPOSS in PFSA must be identified (e.g., sPOSS crosslinking or grafting) or fuel-cell operation must be controlled in such a way as to prevent contact of condensed water with the membrane.

High-water retention, especially at low RH, is an important requirement for sulfonic acid-type PEM fuel cell membranes. At the same time, for acceptable membrane durability in a fuel cell during on/off cycling, there should be minimal in-plane membrane expansion due to water uptake.[13] The PFSA/sPOSS/PAA (60:35:5) membrane possessed an excellent combination of water retention and dimensional stability properties. In-plane (areal) swelling at 80 °C and 90 % RH was 32 %, as compared to 58 % for a homogeneous PFSA/sPOSS (65:35) film. Figure 5 shows the hydration number (H_2O molecules per SO_3H group) as a function of relative humidity at 80 °C for the following: the PFSA/sPOSS/PAA nanofiber composite membrane (based on a polymer IEC of 1.21 and a sPOSS IEC of 4.8, a 60:35 PFSA/sPOSS wt ratio, and a fiber volume fraction of 0.74), a nanofiber PFSA membrane without sPOSS (1.21 IEC, 5 % PAA, 0.71 fiber volume fraction), a 1.21 IEC PFSA recast homogeneous film with 5 % PAA, neat sPOSS, and Nafion 212. The plot was generated from gravimetric water sorption data (see the Supporting Information) and the membrane or sPOSS IEC. The hydration numbers for the individual components that comprise the PFSA/sPOSS/PAA nanofiber composite membrane are all similar in value and equal to those of commercial Nafion over the entire RH range. When PFSA and sPOSS were spun into a nanofiber mat and impregnated with NOA 63, the water uptake changed dramatically, with a substantial increase in the sulfonic acid group waters of hydration. We reason that the unusual and highly desirable water retention behavior of the PFSA/sPOSS/PAA nanofiber film, which has not been observed with other fuel cell membranes, is associated with
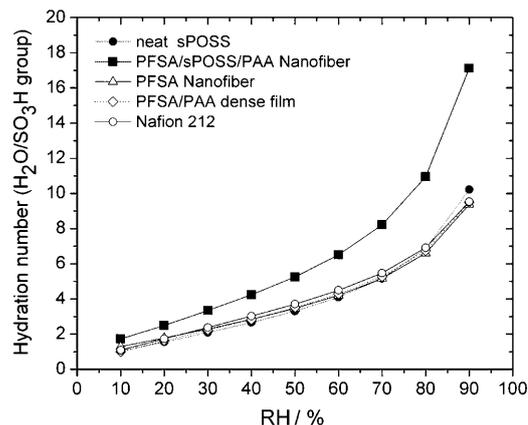
nanovoids within the electrospun fibers which hold water by capillary condensation.[14–16] Such voids do not form when sPOSS is mixed with PFSA and solution cast into a solid dense film (hydration numbers are the same as those for Nafion 212) nor do they form when PFSA is electrospun without sPOSS. The results suggest that the extreme fiber elongation and rapid solvent evaporation during electrospinning create permanent nanovoids within sPOSS microgels or at sPOSS/PFSA interfaces. Clearly, further water uptake analyses are warranted, but at the present time, it can be inferred that the very high proton conductivity of the PFSA/sPOSS/PAA nanofiber composite membrane at low humidities is attributed to the combined effects of a high concentration of sulfonic acid groups and an unusually high number of water molecules hydrating the ion-exchange sites.

Experimental Section

Membrane preparation

Materials: PFSA with an EW of 825 (3M Corporation) and sulfonated octaphenyl polyhedral oligomeric silsesquioxane (sPOSS, Michigan Molecular Institute) were used as proton-conducting components of electrospun nanofibers. Poly(acrylic acid) (viscosity-based molecular weight, $M_v = 450\,000$ g mol^{-1}, Aldrich) was used as the carrier polymer for nanofiber electrospinning. Norland Optical Adhesive (NOA 63) (Norland Products) was used as a pore-filling agent to transform porous nanofiber mats into non-porous, defect-free (fully dense) membranes. Commercial Nafion® (Nafion 212, DuPont) was used as a reference material.

PFSA electrospinning: A series of PFSA/PAA solutions in a 1-propanol/water (2:1 w/w) solvent were prepared, where the total polymer concentration was 5, 10, or 15 wt % and the PAA/PFSA weight ratio varied from 0.05 to 0.50 (5–50 % PAA). Solutions were pumped through a syringe needle (KDS 100 syring pump, KD Scientific) and nanofibers were collected on a stainless steel rotating drum, as described previously.[2] The potential difference between the metallic needle and the drum collector was varied from 6 kV to 12 kV, depending on the electrospinning solution composition. The

spinneret-to-collector distance and flow rate of the solution were fixed at 8 cm and 0.15 mL h^{-1}, respectively. The applied voltage which produced well-formed nanofibers was identified (see Table S1 in the Supporting Information).

PFSA/sPOSS/PAA nanofiber electrospinning: A solution of PFSA/sPOSS/PAA (60:35:5 w/w/w) at a total polymer concentration of 30 wt% in 1-propanol/water (2:1 w/w) was electrospun. The applied potential between the drum collector and the syringe needle was 15 kV, the spinneret-to-collector distance was 8 cm, and the flow rate of polymer solution was 0.15 mL h^{-1}.

PFSA and PFSA/sPOSS nanofiber network composite membrane fabrication: Nanofiber mats of PFSA/PAA (95:5 w/w) and PFSA/sPOSS/PAA (60:35:5 w/w/w) were transformed into non-porous (fully dense) ion-exchange membranes by a series of processing steps. Electrospun mats were first annealed at 140 °C for 5 min under vacuum, during which time intersecting fibers were welded to one another (residual water in the nanofibers plasticized the fibers at the annealing temperature, allowing the polymer to flow and weld). The initial mat had a nanofiber volume fraction of about 0.20. After annealing, the fiber volume fraction increased to 0.40. To further increase the fiber density, annealed mats were mechanically compacted using a hydraulic press (Model: 3912, Carver) Each mat was placed between two Kapton polyimide films and pressed at 69 MPa for 5 s. The voids between fibers in an annealed/compacted mat (fiber volume fraction of 0.71–0.74) were filled with uncharged (hydrophobic) and inert Norland Optical Adhesive (NOA 63), a UV-crosslinkable urethane pre-polymer in liquid form with a low viscosity. A mat was completely immersed in NOA 63 liquid at 45 °C and trapped air (in the mat's pores) was removed by applying a vacuum for 1 h. After impregnation, excess NOA 63 was wiped clean from the mat surfaces and the film was exposed to UV light (365 nm) for 2 h (1 h for each side of the film) for NOA 63 curing. PAA was removed from an impregnated PFSA/PAA nanofiber membrane by boiling the film in 1.0 M H$_2$SO$_4$ and then in deionized water (1 h each). PFSA/sPOSS/PAA nanofiber membranes were not subjected to the acid/water boiling steps.

Membrane characterization

Proton conductivity: In-plane proton conductivity of membranes samples was measured using an AC impedance technique. A 4-probe proton conductivity cell by Bekktech, LLC was employed. Membranes were equilibrated in a temperature/humidity controlled oven (Model: SH-241, ESPEC Corp.) and proton conductivity measured at two temperatures (30 °C and 80 °C) for relative humidities ranging from 20–95%. Conductivities at 120 °C were measured in a similar fashion at Bekktech, LLC.

Water sorption: Equilibrium water vapor uptake by membrane samples was recorded using a dynamic water vapor sorption analyzer (Model: Q5000SA, TA Instruments). Gravimetric water sorption data were collected at two different temperatures (30 °C and 80 °C)

for relative humidities in the 10–90% range. Each sample was predried at 80 °C and 0% RH for 200 min, until the sample weight stabilized (less than 0.001% weight change in 5 min). The testing temperature was set and humidity was increased from 10 to 90% RH and then decreased from 90% to 10% RH at increments of 10% RH. Each sample was equilibrated at a given humidity condition until the weight stabilized (which required at most 100 min). All experiments were run in duplicate; the average error between repeated runs was at most 5%. The hydration number was calculated from the water weight gain, the total dry weight of a membrane sample, the composition of the sample (total dry weight of PFSA and sPOSS), and the IEC of PFSA (1.21 mmol g^{-1}) and sPOSS (4.8 mmol g^{-1}).

[1] N. L. Garland, J. P. Kopasz, *J. Power Sources* **2007**, *172*, 94–99.
[2] J. Choi, K. M. Lee, R. Wycisk, P. N. Pintauro, P. T. Mather, *Macromolecules* **2008**, *41*, 4569–4572.
[3] D. H. Reneker, I. Chun, *Nanotechnology* **1996**, *7*, 216–223.
[4] J. Doshi, D. H. Reneker, *J. Electrost.* **1995**, *35*, 151–160.
[5] F. Dotti, A. Varesano, A. Montarsolo, A. Aluigi, C. Tonin, G. Mazzuchetti, *J. Ind. Text.* **2007**, *37*, 151–162.
[6] eSpin Technologies, www.espintechnologies.com **2010**.
[7] B. Bae, T. Yoda, K. Miyatake, H. Uchida, M. Watanabe, *Angew. Chem.* **2010**, *122*, 327–330; *Angew. Chem. Int. Ed.* **2010**, *49*, 317–320.
[8] G. Maier, J. Meier-Haack, *Fuel Cells II* **2008**, *216*, 1–62.
[9] A. Laforgue, L. Robitaille, A. Mokrini, A. Ajji, *Macromol. Mater. Eng.* **2007**, *292*, 1229–1236.
[10] H. Chen, J. D. Snyder, Y. A. Elabd, *Macromolecules* **2008**, *41*, 128–135.
[11] C. Nah, Y.-S. Lee, B. H. Cho, H. C. Yu, B. Akle, D. J. Leo, *Compos. Sci. Technol.* **2008**, *68*, 2960–2964.
[12] Y.-W. Chang, E. Wang, G. Shin, J.-E. Han, P. T. Mather, *Polym. Adv. Technol.* **2007**, *18*, 535–543.
[13] H. Tang, S. Peikang, S. P. Jiang, F. Wang, M. Pan, *J. Power Sources* **2007**, *170*, 85–92..
[14] S. Megelski, J. S. Stephens, D. B. Chase, J. F. Rabolt, *Macromolecules* **2002**, *35*, 8456–8466.
[15] X-M. Yan, P. Mei, Y. Mi, L. Gao, S. Qin, *Electrochem. Commun.* **2009**, *11*, 71–74.
[16] M. J. Park, K. H. Downing, A. Jackson, E. D. Gomez, A. M. Minor, D. Cookson, A. Z. Weber, N. P. Balsara, *Nano Lett.* **2007**, *7*, 3547–3552.